ABHD16A deficiency causes a complicated form of hereditary spastic paraplegia associated with intellectual disability and cerebral anomalies

Gabrielle Lemire,[1,2,19,*] Yoko A. Ito,[1,19] Aren E. Marshall,[1] Nicolas Chrestian,[3,4] Valentina Stanley,[5] Lauren Brady,[6] Mark Tarnopolsky,[6] Cynthia J. Curry,[7] Taila Hartley,[1] Wendy Mears,[1] Alexa Derksen,[8,9] Nadie Rioux,[4] Nataly Laflamme,[4] Harrol T. Hutchison,[10] Lynn S. Pais,[2] Maha S. Zaki,[11] Tipu Sultan,[12] Adrie D. Dane,[13] Care4Rare Canada Consortium, Joseph G. Gleeson,[5] Frédéric M. Vaz,[14,15,16] Kristin D. Kernohan,[1,17] Geneviève Bernard,[8,9,18,20] and Kym M. Boycott[1,20,*]

Summary

ABHD16A (abhydrolase domain-containing protein 16A, phospholipase) encodes the major phosphatidylserine (PS) lipase in the brain. PS lipase synthesizes lysophosphatidylserine, an important signaling lipid that functions in the mammalian central nervous system. *ABHD16A* has not yet been associated with a human disease. In this report, we present a cohort of 11 affected individuals from six unrelated families with a complicated form of hereditary spastic paraplegia (HSP) who carry bi-allelic deleterious variants in *ABHD16A*. Affected individuals present with a similar phenotype consisting of global developmental delay/intellectual disability, progressive spasticity affecting the upper and lower limbs, and corpus callosum and white matter anomalies. Immunoblot analysis on extracts from fibroblasts from four affected individuals demonstrated little to no ABHD16A protein levels compared to controls. Our findings add *ABHD16A* to the growing list of lipid genes in which dysregulation can cause complicated forms of HSP and begin to describe the molecular etiology of this condition.

Hereditary spastic paraplegias (HSPs) comprise a broad and diverse group of inherited neurodevelopmental or neurodegenerative disorders in which the main neurological symptom is progressive lower limb spasticity and weakness. HSPs are genetically heterogeneous with approximately 80 suspected genetic subtypes and more than 60 genes identified to date; autosomal-dominant, autosomal-recessive, and X-linked modes of inheritance have all been described.[1,2] HSPs were historically clinically classified as isolated or complicated; complicated HSP presents with additional neurological or extra-neurological signs such as intellectual disability, cerebellar dysfunction, neuropathy, or ophthalmological anomalies.[3] Advances in genomic technologies have revealed significant clinical and genetic overlap within different HSP subtypes and between HSP and other neurodegenerative diseases, such as Charcot-Marie-Tooth neuropathy.[4,5]

Many HSP-associated genes have been found to alter lipid metabolism and homeostasis, highlighting the importance of these processes in neuronal physiology. Pathogenic variants in genes encoding various enzymes involved in the metabolism and the inter-organellar trafficking of different lipid classes, including cholesterols, phospholipids, sphingolipids, and fatty acids, have been associated with HSP (reviewed in Darios et al.[6]). Alterations of lipid metabolism are postulated to be contributing factors that lead to the degeneration of axons and, thus, are involved in the underlying pathophysiology of HSP.

In this study, we present a cohort of individuals affected with a progressive neurological condition who all harbor

[1]Children's Hospital of Eastern Ontario Research Institute, University of Ottawa, Ottawa, ON K1H 8L1, Canada; [2]Broad Center for Mendelian Genomics, Program in Medical and Population Genetics, Broad Institute of MIT and Harvard, Cambridge, MA 02142, USA; [3]Department of Paediatric Neurology, Paediatric Neuromuscular Disorder, Centre Mère Enfant Soleil, Laval University, Quebec City, QC G1V 4G2, Canada; [4]Department of Molecular Medicine, Faculty of Medicine, Neuroscience Laboratory, CHU de Québec Research Center, Laval University, Quebec City, QC G1V 4G2, Canada; [5]Laboratory for Pediatric Brain Disease, Rady Children's Institute for Genomic Medicine, University of California, San Diego, San Diego, CA 92093, USA; [6]Neuromuscular and Neurometabolics Division, Department of Pediatrics, McMaster University, Hamilton, ON L8N 3Z5, Canada; [7]Genetic Medicine Division, Department of Pediatrics, University of California, San Francisco, Fresno, CA 93701, USA; [8]Child Health and Human Development Program, McGill University Health Centre Research Institute, Montréal, QC H4A 3J1, Canada; [9]Departments of Neurology and Neurosurgery, Pediatrics and Human Genetics, McGill University, Montreal, QC H3A 0G4, Canada; [10]Neurology Division, Department of Pediatrics, University of California, San Francisco, Fresno, CA 93701, USA; [11]Clinical Genetics Department, Human Genetics and Genome Research Division, National Research Centre, 12311 Cairo, Egypt; [12]Department of Pediatric Neurology, Institute of Child Health, Children Hospital Lahore, 54000 Lahore, Pakistan; [13]Bioinformatics Laboratory, Department of Epidemiology and Data Science, Amsterdam Public Health Research Institute, Amsterdam UMC, University of Amsterdam, Amsterdam 1105, the Netherlands; [14]Laboratory Genetic Metabolic Diseases, Amsterdam UMC, University of Amsterdam, Departments of Clinical Chemistry and Pediatrics, Amsterdam Gastroenterology and Endocrinology Metabolism, Amsterdam 1105, the Netherlands; [15]Department of Pediatrics, Emma Children's Hospital, Amsterdam UMC, University of Amsterdam, Amsterdam 1105, the Netherlands; [16]Core Facility Metabolomics, Amsterdam UMC, Amsterdam 1105, the Netherlands; [17]Newborn Screening Ontario, Children's Hospital of Eastern Ontario, Ottawa, ON K1H 8L1, Canada; [18]Department of Specialized Medicine, Division of Medical Genetics, McGill University Health Center, Montreal, QC H4A 3J1, Canada
[19]These authors contributed equally
[20]These authors contributed equally
*Correspondence: glemire@cheo.on.ca (G.L.), kboycott@cheo.on.ca (K.M.B.)
https://doi.org/10.1016/j.ajhg.2021.09.005.
© 2021 American Society of Human Genetics.

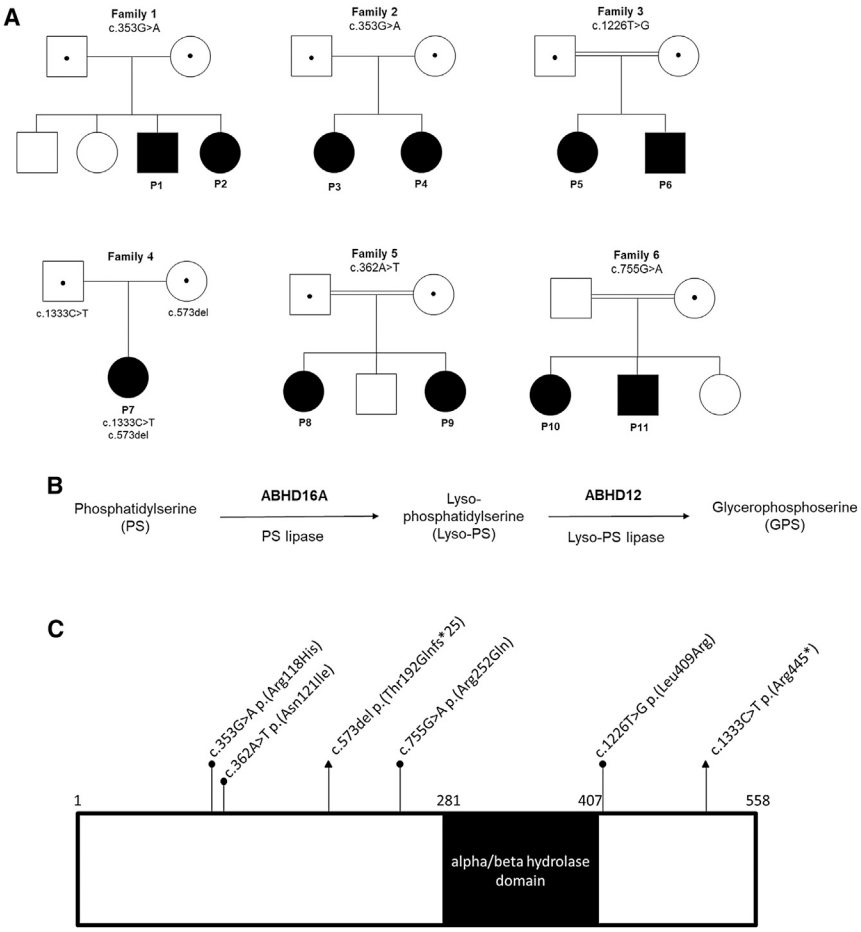

Figure 1. Pedigree and summary of *ABHD16A* variants

(A) Pedigree of the six families with variants in *ABHD16A*, showing consanguinity in three families. Black symbols represent affected individuals. Symbols containing a dot represent a heterozygous carrier status confirmed in an adult. Unaffected siblings were all confirmed to not be homozygous for the variant present in the family.
(B) Schematic of phosphatidylserine (PS) lipase and lysophosphatidylserine (lyso-PS) lipase activities by ABHD16A and ABHD12.
(C) Representation of the six variants in *ABHD16A* (GenBank: NM_021160.2) present in the 11 affected individuals. This transcript encodes a protein that is 558 amino acids in length.

bi-allelic variants in abhydrolase domain-containing protein 16A, phospholipase *(ABHD16A* [MIM: 142620]). *ABHD16A* encodes the major phosphatidylserine (PS) lipase in the brain, which synthesizes the signaling lipid lysophosphatidylserine (lyso-PS).[7] To our knowledge, *ABHD16A* has not previously been linked to any genetic disorder.

ABHD16A was initially identified as a compelling novel candidate gene in affected sibling pairs from two French-Canadian families (individuals P1 and P2 from family 1 and individuals P3 and P4 from family 2, Figure 1A). The affected individuals presented with intellectual disability and progressive spasticity of the upper and lower limbs (Tables 1 and S1). Cerebral MRIs revealed a thin corpus callosum and white matter anomalies (Figure 2). Three of these individuals also presented with an axonal neuropathy, and one had myoclonic seizures. Although the two families were not known to be related to each other, their exome sequencing data were investigated together because of their ethnicity and similar clinical presentation. Exome sequencing of the two affected sibling pairs, performed as part of the Care4Rare Canada research program,[8] identified a homozygous c.353G>A (p.Arg118His) variant in *ABHD16A* (GenBank: NM_021160.2) in all four affected individuals (P1, P2, P3, and P4). Interestingly, this variant was not called by an older version of the Care4Rare bioinformatics pipeline. The c.353G>A variant occurs at a highly conserved site (PhyloP score of 4.56). This variant is rare in gnomAD v.2.1.1, having only two alleles identified (2/246,600 alleles) and an allele frequency of 0.0008%.[9] *In silico* prediction programs, including CADD, MutationTaster, SIFT, and PolyPhen-2, all predict this missense change to have a deleterious effect on ABHD16A. Sanger sequencing confirmed that each parent in families 1 and 2 was heterozygous for the c.353G>A variant and that the variant was present in the homozygous state in the four affected individuals. Also, the two unaffected children in family 1 were shown to not be homozygous for the c.353G>A variant. ABHD16A is the major phospholipase in the brain that converts PS to lyso-PS (Figure 1B).[7] Lyso-PS is present in all tissues but is most abundant in the central nervous system and immune cells where it is postulated to regulate numerous immunological and neurological processes.[10] For instance, lyso-PS is involved in the regulation of macrophage activation, clearance of apoptotic cells, human cancer cell migration, and glucose metabolism in the brain and skeletal muscles.[11–15] Given the evidence above, the homozygous variant in *ABHD16A* was deemed to be a strong candidate for causing the HSP phenotype in the two sibling pairs.

We next sought to identify additional affected individuals by using the internal Care4Rare database, Matchmaker Exchange (MME),[16] and Geno2MP. Within the internal Care4Rare database, we identified potentially deleterious variants in *ABHD16A* in three additional individuals (P5, P6, and P7) from two unrelated families with a similar HSP phenotype (Table 1, Figure 1A, and Table S1). The first two affected individuals (P5 and P6, Figure 1A) were siblings from a consanguineous Armenian family (family 3). Similar to the affected individuals in families 1 and 2, individuals P5 and P6 presented with

Table 1. Clinical features of 11 individuals from six families with bi-allelic variants in *ABHD16A*

Family	**1**		**2**		**3**		**4**	**5**		**6**	
Variant in *ABHD16A*[a]	c.353G>A		c.353G>A		c.1226T>G		c.1333C>T; c.573delG	c.362A>T		c.755G>A	
Protein change	p.Arg118His		p.Arg118His		p.Leu409Arg		p.Arg445*; p.Thr192Glnfs*25	p.Asn121Ile		p.Arg252Gln	
Zygosity	homozygous		homozygous		homozygous		compound heterozygous	homozygous		homozygous	
Ethnicity	French-Canadian		French-Canadian		Armenian		Mixed European	Egyptian		Pakistani	
Consanguinity	–		–		+		–	+		+	
Individual	**1**	**2**	**3**	**4**	**5**	**6**	**7**	**8**	**9**	**10**	**11**
Sex (M/F)[b]	M	F	F	F	F	M	F	F	F	F	M
Age (years)[c]	12	11	14	16	21	10	5	21	12	16	12
ID/GDD[d]	+	+	+	+	+	+	+	+	+	+	+
Upper limb spasticity	+	+	+	+	+	+	–	–	–	–	+
Joint contractures	+	+	+	+	+	+	–	–	–	+	+
Neuropathy	–	+	+	+	U[e]	U[e]	U[e]	U[e]	U[e]	U[e]	U[e]
Seizures	+	–	–	–	–	+	–	–	–	–	–
Thin corpus callosum	+	+	+	+	+	+	+	+	+	–	–
White matter anomalies	+	+	+	+	+	+	+	+	–	+	+
Behavioral anomalies[f]	–	–	–	–	–	+	+	–	–	–	–

[a]GenBank: NM_021160.2.
[b]M, male; F, female.
[c]Age at time of publication.
[d]ID, intellectual disability; GDD, global developmental delay.
[e]U, unknown (EMG/NCS was not performed in these individuals).
[f]Autism spectrum disorder, self-injurious behaviors.

intellectual disability, progressive spasticity of upper and lower limbs, white matter anomalies, and a thin corpus callosum (Figure 2). SNP array revealed several long contiguous stretches of homozygosity greater than 5 Mb in size, estimated to encompass approximately 5.7% of the autosome genome, which is consistent with the parents' being reported as first cousins. Exome sequencing identified a homozygous c.1226T>G (p.Leu409Arg) missense variant in *ABHD16A* in both individuals P5 and P6. Similar to the exome data for families 1 and 2, the variants in *ABHD16A* were only called in the updated version of the Care4Rare bioinformatics pipeline. This c.1226T>G variant is absent from gnomAD[9] and occurs at a highly conserved site (PhyloP score of 4.16), and *in silico* prediction software predict this missense change to have a deleterious impact on ABHD16A. Sanger sequencing confirmed that each parent was heterozygous for the c.1226T>G variant and that the variant was present in the homozygous state in the two affected siblings. The final individual identified in the Care4Rare database was individual P7 from family 4 (Figure 1A), who was compound heterozygous for a c.1333C>T (p.Arg445*) variant and a c.573del (p.Thr192Glnfs*25) variant in *ABHD16A*. This patient presented with hypotonia, severe global developmental delay, and progressive lower limb spasticity (Tables 1 and S1). Her cerebral MRI revealed a thin corpus callosum and white matter anomalies (Figure 2). The paternally inherited c.1333C>T variant was a nonsense variant predicted to result in a premature stop codon at amino acid position 445 located in exon 16. The c.1333C>T variant is rare in gnomAD v.2.1.1, having only one allele identified (1/247,968 alleles and an allele frequency of 0.0004%).[9] The c.573del variant was maternally inherited and absent from gnomAD.[9] The deletion of the single G nucleotide is predicted to cause a frameshift at amino acid position 192 located in exon 7 and a premature stop codon at amino acid position 217.

The Geno2MP database was interrogated for *ABHD16A* variants linked to individuals with the Human Phenotype Ontology (HPO) term "abnormality of the nervous system" (Geno2MP accessed in April 2020). Through this one-sided matchmaking strategy, two additional sets of siblings (individuals P8 and P9 from family 5 and individuals P10 and P11 from family 6) were identified as having potentially deleterious variants in *ABHD16A*. Collaborative discussions revealed that the affected individuals from both families had a remarkably similar clinical presentation to the aforementioned individuals (Tables 1 and S1). Individuals P8 and P9 (family 5, Figure 1A). were affected sisters from a consanguineous Egyptian family. A homozygous c.362A>T (p.Asn121Ile) missense variant in *ABHD16A* was identified by exome sequencing as a potential novel candidate gene and submitted to the Geno2MP database. The c.362A>T variant is absent from gnomAD[9]

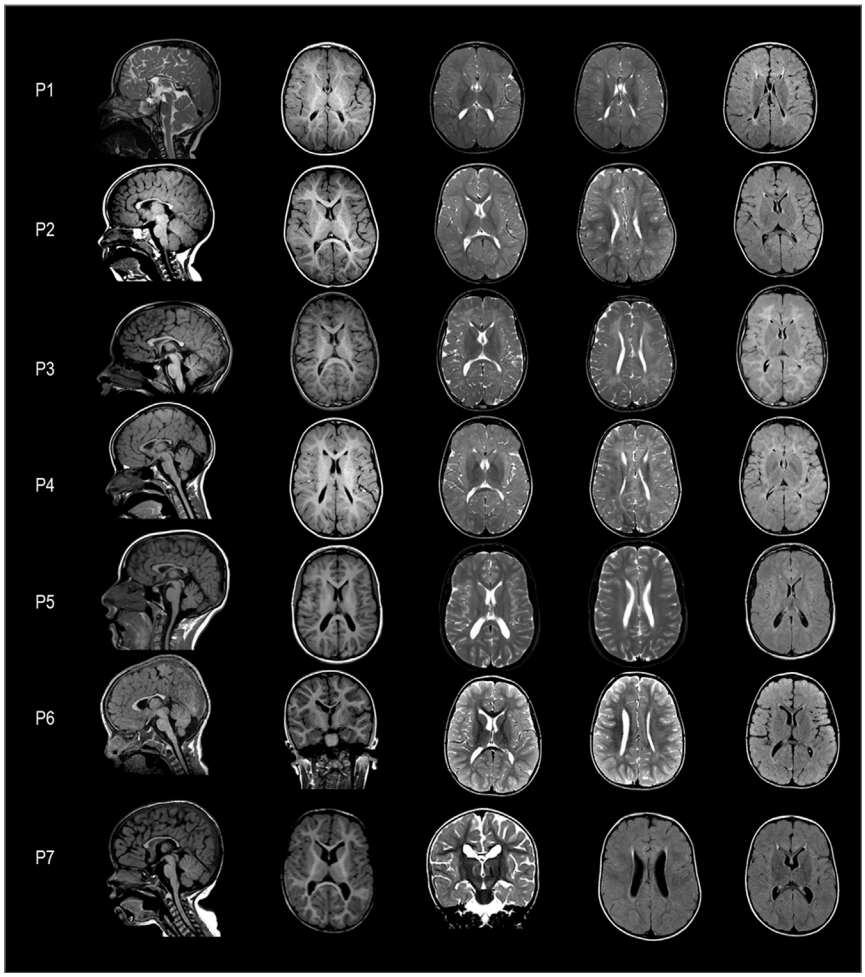

Figure 2. Brain MRI characteristics of individuals P1–P7
The MRIs were performed at the following ages: P1, 3 years 3 months; P2, 2 years 3 months; P3, 12 years 3 months; P4, 9 years 4 months; P5, 19 years 3 months; P6, 3 years 9 months; and P7, 26 months. From left to right, sagittal midline, axial T1 (except P6, coronal), axial T2 (except P7, coronal) at the level of basal ganglia, axial T2 (except P7, FLAIR) at the level of the lateral ventricles, and axial FLAIR at the level of the basal ganglia. Affected individuals with bi-allelic variants in *ABHD16A* have a thin corpus callosum (first column), with or without cavum vergae and/or cavum septum pellucidum (columns 2, 3, and 5), and non-specific periventricular and/or deep white matter abnormalities (columns 3, 4, and 5).

and occurs at a moderately conserved site (PhyloP score of 3.76), and *in silico* programs predict this missense change to have a deleterious effect on protein function. Family segregation studies confirmed that individuals P8 and P9 were homozygous for the c.362A>T variant and indicated that each parent was heterozygous for the c.362A>T variant and that the unaffected sibling did not carry the variant in the homozygous state. Finally, individuals P10 and P11 (family 6, Figure 1A) were affected siblings from a consanguineous Pakistani family. A homozygous c.755G>A (p.Arg252Gln) missense variant was identified by exome sequencing in the two affected individuals as a potential novel candidate gene and submitted to the Geno2MP database. The c.755G>A variant is absent from gnomAD[9] and occurs at a highly conserved site (PhyloP score of 5.61), and *in silico* programs predict this missense change to have a deleterious effect on protein function. Follow-up studies by Sanger sequencing confirmed that individuals P10 and P11 were homozygous for the c.755G>A variant, their mother was heterozygous for the variant, and the unaffected sibling did not carry the variant in the homozygous state.

In summary, exome sequencing combined with a one-sided matchmaking strategy resulted in the assembly of a cohort of six unrelated families with 11 affected individuals having bi-allelic variants in *ABHD16A* and presenting with a complicated form of HSP. No other variants in disease-associated or novel genes were retained as plausible candidates by exome analysis for any of the affected individuals. The phenotypic overlap between the 11 affected individuals is striking because they all present with variable degrees of developmental delay/intellectual disability and progressive spasticity affecting predominantly the lower limbs. The mean age of onset of the lower limb spasticity in individuals from this cohort was 3 years old, and the spasticity progressively became worse over time (Table S1). In addition, almost all individuals presented with corpus callosum and white matter anomalies. The identified variants in *ABHD16A* were very compelling given their deleterious *in silico* predictions, their rarity in population data, and the involvement of ABHD16A in lipid metabolism, a key process in neuronal physiology.

Next, we performed functional studies to investigate for additional evidence of causality. We began by evaluating the impact of the *ABHD16A* variants on overall ABHD16A expression in primary fibroblast cells from the affected individuals P3, P4, P7, and P9. Real-time PCR data revealed cells from P3 and P9 did not have significantly different *ABHD16A* mRNA transcript abundance compared to control fibroblasts, while fibroblast cells from P4 had a significant increase compared to controls but was not significantly different from P3 and P9 (Figure 3A). On the other hand, P7 had a significant decrease in *ABHD16A* mRNA transcript abundance compared to all other samples, which was not unexpected because this individual is compound heterozygous for a nonsense and a frameshift variant; all other affected individuals harbor missense

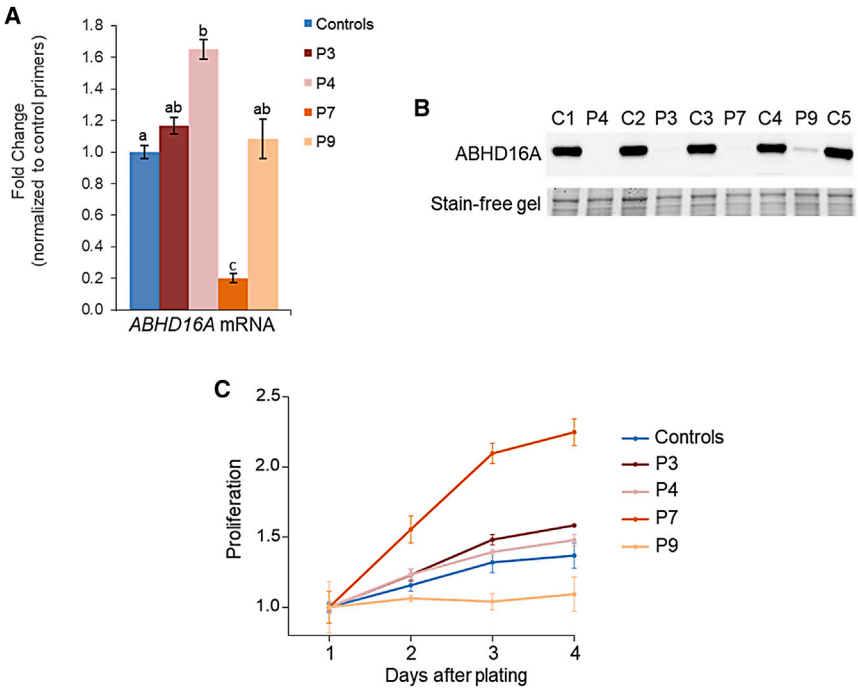

Figure 3. Bi-allelic *ABHD16A* variants result in decreased ABHD16A expression in fibroblast cells from affected individuals
(A) Real-time PCR analysis on cDNA from affected individual fibroblast cells showing *ABHD16A* transcript levels in affected cells compared to controls. Letters above error bars denote statistical significance ($p < 0.05$) as determined by one-way analysis of variance (ANOVA) and Tukey's multiple-comparison test; samples with the same letter are not significantly different.
(B) Immunoblot analysis on extracts from affected individual fibroblast cells showing little to no ABHD16A expression in affected cells compared to controls.
(C) Cell proliferation of control and affected fibroblast cells was measured via assessment of cell confluency on each of the specified days after initial plating. For each of the panels in this figure, five control cell lines were used and the mean data were graphed; all error bars depict standard error of the mean.

variants (Figure 3A and Table 1). Immunoblot analysis of whole fibroblast cell extracts demonstrated little to no ABHD16A in all tested affected individuals compared to controls (Figure 3B). The ABHD16A antibody used for this study targets the C-terminal end of ABHD16A and is thus predicted to not detect the p.Thr192Glnfs*21 mutant protein. Also, because it is not known whether the epitope is present before or after amino acid position 445, the ability of this antibody to detect the p.Arg445* mutant protein is not known. Nevertheless, on the basis of the real-time PCR results, which showed significant reduction of ABHD16A mRNA in P7 fibroblast cells, the mutant protein levels in this affected individual would be predicted to also be significantly reduced. Finally, we investigated the effect of drastically reduced ABHD16A protein levels on cellular proliferation. We determined that fibroblasts from the affected individuals have a broad range of proliferation compared to controls (Figure 3C).

Given the role of ABHD16A in synthesizing lyso-PS, the effects of the *ABHD16A* variants on lipid metabolism were investigated via cultured patient fibroblasts and plasma samples. Lipidomic studies in fibroblasts unexpectedly did not reveal a clear change in lyso-PS levels in affected individual fibroblasts (P3, P4, P7, and P9) relative to control fibroblasts; PS levels were elevated, but lyso-PS levels were not decreased (Figure S1). A similar observation was made in plasma samples collected from patients (P1, P2, P3, and P4) when compared to unaffected heterozygous family members (parents and unaffected sibling; data not shown). Other lipidomic changes in fibroblasts were observed, suggesting that ABHD16A may be involved in regulating the lipidome through other pathways (Figure S1). To date, the characterization of ABHD16A has largely focused on confirming its enzymatic function in converting intracellular PS to lyso-PS in the brain and spinal cord.[7] Therefore, although ABHD16A PS lipase activity has been detected *in vitro* in some non-neuronal human cell lines, mainly lymphoblast and cancer cell lines, its activity in most non-neuronal cells, including fibroblasts, is currently unknown.[7] The presence of other PS lipases in fibroblasts could also be a reason that no disturbances were found in lyso-PS levels. Moreover, the biological function of lyso-PS synthesized by ABHD16A in non-neuronal cells is currently unknown. Of note, lipidomic studies on brain tissue from a deceased individual with Sjögren-Larsson syndrome, another neurometabolic disorder, have been shown to give invaluable insight into the lipid profile of an affected tissue and to differ significantly from the profile seen in plasma and fibroblasts.[17] The lipidomic analyses performed in the current study were limited to skin and plasma, raising the possibility that lipidomic profiling of central nervous system tissues may give very different results.

As shown in Figure 1B, *ABHD12* encodes a lipase that degrades lyso-PS and, thus, functions downstream of *ABHD16A*. Bi-allelic pathogenic variants in *ABHD12* are associated with the neurological disorder PHARC (polyneuropathy, hearing loss, ataxia, retinitis pigmentosa, and cataract [MIM: 612674]).[18,19] In PHARC, dysfunction of the ABHD12 lyso-PS lipase leads to an accumulation of lyso-PS in the brain, which is postulated to result in microglial activation and motor defects.[19] Surprisingly, *Abhd16a*-null mice do not appear to have postnatal central nervous system anomalies despite having reduced levels of lyso-PS.[7] Because the *Abhd16a*-null mice were assessed until 10 weeks after birth, the development of central

nervous system anomalies after this time point remains a possibility. However, there appears to be an increased incidence of prenatal lethality, and the *Abhd16a*-null mice that were born were 30% smaller in size compared to their wild-type littermates.[7] More research is required to elucidate the different roles that lyso-PS plays in different species and tissues as well as during different stages of development. In addition, differences in several lipid species were observed between affected individual and control fibroblasts, including phosphatidylcholine (PC), akylphosphatidylethanolamine (PC[O]), and alkenylphosphatidylcholine (PC[P]), and to a lesser extent their ethanolamine counterparts (Figure S1), raising the possibility that ABHD16A is involved in additional routes of lipid metabolism. Nevertheless, the association of *ABHD16A* and *ABHD12* with distinct neurological disorders in humans highlights the importance of this pathway in maintaining the normal function of the post-natal human central nervous system.

ABHD16A is located on chromosome 6p21.33, and its most abundant transcript (GenBank:NM_021160.2) consists of 20 exons that encode a protein that is 558 amino acids in length. ABHD16A belongs to the ABHD superfamily of proteins that share an α/β-hydrolase fold.[20] Collectively, four missense variants, one nonsense variant, and one frameshift variant were identified through exome sequencing in affected individuals from this study. Interestingly, the six variants are located throughout the gene and do not cluster to any particular region (Figure 1C). In fact, none of the four missense variants localize to the α/β-hydrolase domain or to any of the predicted conserved nucleophilic or acetyltransferase motifs.[21,22] Although the variants identified in this study occur throughout *ABHD16A*, the c.353G>A variant was identified in the two unrelated sibling pairs of French-Canadian descent, raising the possibility that this particular variant is a founder mutation in the French-Canadian population. A shared haplotype on chromosome 6 ((chr6: 29,709,714–32,522,379(hg19)) with the variant in *ABHD16A* located at chr6: 31,664,801(hg19)) was identified in the four affected individuals and the two sets of parents from families 1 and 2, supporting that this variant was inherited from a common ancestor.

Interestingly, the *ABHD16A* variants in families 1, 2, and 3 were only called after the exome data were rerun with an updated version of the Care4Rare bioinformatics pipeline (version 2.0) and had been missed during the first exome analyses performed prior to 2017. Thus far, we have been unsuccessful in determining why they were previously missed. We know that the variants were not included in the original variant calling files, but we did not identify any overt issues with either our alignment or our calling that would explain why this was the case. *ABHD16A* has no known pseudogenes that might increase the risk of mapping errors. This gene currently has ample coverage in public databases such as gnomAD, and our updated pipeline, as well as the Broad Institute pipeline (which sequenced families 5 and 6 in this cohort), had no issues identifying variants in *ABHD16A* in their most recent iteration. In addition, on the basis of our 5 years of experience with MME, we were very surprised that no matches were made via this platform, which again suggests variants in this gene might have been missed in the past by other pipelines. *ABHD16A*-associated complicated HSP might thus be a more frequently occurring condition than is currently acknowledged. We recommend that molecular geneticists confirm the inclusion of *ABHD16A* in their variant calling files, particularly when investigating individuals with complex HSP.

In conclusion, our findings support that bi-allelic deleterious variants in *ABHD16A* cause an autosomal-recessive subtype of complicated HSP. ABHD16A PS lipase deficiency results in intellectual disability, progressive spasticity, abnormal corpus callosum, and white matter anomalies, most likely through the dysregulation of lipid species including lyso-PS. The identification of *ABHD16A* as an HSP gene again demonstrates the crucial role that lipid metabolism and homeostasis have in maintaining the nervous system. Importantly, because this disorder is an inborn error of lipid metabolism and has a progressive course, research is needed to investigate whether affected individuals could benefit from pharmacological, or other, intervention. Finally, this multi-center study highlights the importance of sharing genomic data for the identification of novel genes in rare disorders such as HSP.

Data and code availability

The *ABHD16A* variants were submitted to ClinVar (https://www.ncbi.nlm.nih.gov/clinvar/) (GenBank: NM_021160.2; accession numbers SCV001787122, SCV001787123, SCV001787124, SCV001787125, SCV001787126, and SCV001787127). The exome datasets supporting this study have not been deposited in a public repository because of ethical restriction but are available from the corresponding author on request.

Supplemental information

Supplemental information can be found online at https://doi.org/10.1016/j.ajhg.2021.09.005.

Acknowledgments

We thank the families for their participation. This work was performed under the Care4Rare Canada Consortium funded by Genome Canada and the Ontario Genomics Institute (OGI-147), the Canadian Institutes of Health Research, Ontario Research Fund, Genome Alberta, Genome British Columbia, Genome Quebec, Children's Hospital of Eastern Ontario Foundation, and the Fondation Leucodystrophie. G.L. was supported by a CHAMO (Children's Hospital Academic Medical Organization) clinical fellowship award through the Children's Hospital of Eastern Ontario. A.E.M. was supported by a CIHR fellowship award (MFE-176616). K.M.B. was supported by a CIHR Foundation Grant (FDN-154279) and a Tier 1 Canada Research Chair in Rare Disease Precision Health. G.B. has received a Research Scholar Junior 1 award from the Fonds de Recherche du Quebec – Santé (FRQS) (2012-2016), the New Investigator Salary Award from the Canadian Institutes of Health Research (2017-2022), and a Research

Scholar Senior award from the FRQS (2022-2025). Sequencing and analysis were in part provided by the Broad Institute of MIT and Harvard Center for Mendelian Genomics (Broad CMG) and was funded by the National Human Genome Research Institute, the National Eye Institute, and the National Heart, Lung, and Blood Institute grant UM1 HG008900 and in part by National Human Genome Research Institute grant R01 HG009141.

Declaration of interests

The authors declare no competing interests.

Received: July 22, 2021
Accepted: September 8, 2021
Published: September 28, 2021

Web resources

CADD, https://cadd.gs.washington.edu/
Geno2MP, https://geno2mp.gs.washington.edu/
gnomAD, https://gnomad.broadinstitute.org/
Mutation Taster, http://www.mutationtaster.org/
OMIM, https://omim.org
PolyPhen2, http://genetics.bwh.harvard.edu/pph2/
SIFT, https://sift.bii.a-star.edu.sg/

References

1. Tesson, C., Koht, J., and Stevanin, G. (2015). Delving into the complexity of hereditary spastic paraplegias: how unexpected phenotypes and inheritance modes are revolutionizing their nosology. Hum. Genet. *134*, 511–538.
2. Klebe, S., Stevanin, G., and Depienne, C. (2015). Clinical and genetic heterogeneity in hereditary spastic paraplegias: from SPG1 to SPG72 and still counting. Rev. Neurol. (Paris) *171*, 505–530.
3. Harding, A.E. (1983). Classification of the hereditary ataxias and paraplegias. Lancet *1*, 1151–1155.
4. Timmerman, V., Clowes, V.E., and Reid, E. (2013). Overlapping molecular pathological themes link Charcot-Marie-Tooth neuropathies and hereditary spastic paraplegias. Exp. Neurol. *246*, 14–25.
5. Pensato, V., Castellotti, B., Gellera, C., Pareyson, D., Ciano, C., Nanetti, L., Salsano, E., Piscosquito, G., Sarto, E., Eoli, M., et al. (2014). Overlapping phenotypes in complex spastic paraplegias SPG11, SPG15, SPG35 and SPG48. Brain *137*, 1907–1920.
6. Darios, F., Mochel, F., and Stevanin, G. (2020). Lipids in the Physiopathology of Hereditary Spastic Paraplegias. Front. Neurosci. *14*, 74.
7. Kamat, S.S., Camara, K., Parsons, W.H., Chen, D.H., Dix, M.M., Bird, T.D., Howell, A.R., and Cravatt, B.F. (2015). Immunomodulatory lysophosphatidylserines are regulated by ABHD16A and ABHD12 interplay. Nat. Chem. Biol. *11*, 164–171.
8. Beaulieu, C.L., Majewski, J., Schwartzentruber, J., Samuels, M.E., Fernandez, B.A., Bernier, F.P., Brudno, M., Knoppers, B., Marcadier, J., Dyment, D., et al. (2014). FORGE Canada Consortium: outcomes of a 2-year national rare-disease gene-discovery project. Am. J. Hum. Genet. *94*, 809–817.
9. Karczewski, K.J., Francioli, L.C., Tiao, G., Cummings, B.B., Alföldi, J., Wang, Q., Collins, R.L., Laricchia, K.M., Ganna, A., Birnbaum, D.P., et al. (2020). The mutational constraint spectrum quantified from variation in 141,456 humans. Nature *581*, 434–443.
10. Singh, S., Joshi, A., and Kamat, S.S. (2020). Mapping the Neuroanatomy of ABHD16A, ABHD12, and Lysophosphatidylserines Provides New Insights into the Pathophysiology of the Human Neurological Disorder PHARC. Biochemistry *59*, 2299–2311.
11. Frasch, S.C., and Bratton, D.L. (2012). Emerging roles for lysophosphatidylserine in resolution of inflammation. Prog. Lipid Res. *51*, 199–207.
12. Frasch, S.C., Fernandez-Boyanapalli, R.F., Berry, K.A., Murphy, R.C., Leslie, C.C., Nick, J.A., Henson, P.M., and Bratton, D.L. (2013). Neutrophils regulate tissue Neutrophilia in inflammation via the oxidant-modified lipid lysophosphatidylserine. J. Biol. Chem. *288*, 4583–4593.
13. Yea, K., Kim, J., Lim, S., Kwon, T., Park, H.S., Park, K.S., Suh, P.G., and Ryu, S.H. (2009). Lysophosphatidylserine regulates blood glucose by enhancing glucose transport in myotubes and adipocytes. Biochem. Biophys. Res. Commun. *378*, 783–788.
14. Lee, S.Y., Lee, H.Y., Kim, S.D., Jo, S.H., Shim, J.W., Lee, H.J., Yun, J., and Bae, Y.S. (2008). Lysophosphatidylserine stimulates chemotactic migration in U87 human glioma cells. Biochem. Biophys. Res. Commun. *374*, 147–151.
15. Iida, Y., H Tsuno, N., Kishikawa, J., Kaneko, K., Murono, K., Kawai, K., Ikeda, T., Ishihara, S., Yamaguchi, H., Sunami, E., et al. (2014). Lysophosphatidylserine stimulates chemotactic migration of colorectal cancer cells through GPR34 and PI3K/Akt pathway. Anticancer Res. *34*, 5465–5472.
16. Philippakis, A.A., Azzariti, D.R., Beltran, S., Brookes, A.J., Brownstein, C.A., Brudno, M., Brunner, H.G., Buske, O.J., Carey, K., Doll, C., et al. (2015). The Matchmaker Exchange: a platform for rare disease gene discovery. Hum. Mutat. *36*, 915–921.
17. Staps, P., Rizzo, W.B., Vaz, F.M., Bugiani, M., Giera, M., Heijs, B., van Kampen, A.H.C., Pras-Raves, M.L., Breur, M., Groen, A., et al. (2020). Disturbed brain ether lipid metabolism and histology in Sjögren-Larsson syndrome. J. Inherit. Metab. Dis. *43*, 1265–1278.
18. Fiskerstrand, T., H'mida-Ben Brahim, D., Johansson, S., M'zahem, A., Haukanes, B.I., Drouot, N., Zimmermann, J., Cole, A.J., Vedeler, C., Bredrup, C., et al. (2010). Mutations in ABHD12 cause the neurodegenerative disease PHARC: An inborn error of endocannabinoid metabolism. Am. J. Hum. Genet. *87*, 410–417.
19. Blankman, J.L., Long, J.Z., Trauger, S.A., Siuzdak, G., and Cravatt, B.F. (2013). ABHD12 controls brain lysophosphatidylserine pathways that are deregulated in a murine model of the neurodegenerative disease PHARC. Proc. Natl. Acad. Sci. USA *110*, 1500–1505.
20. Ollis, D.L., Cheah, E., Cygler, M., Dijkstra, B., Frolow, F., Franken, S.M., Harel, M., Remington, S.J., Silman, I., Schrag, J., et al. (1992). The alpha/beta hydrolase fold. Protein Eng. *5*, 197–211.
21. Lord, C.C., Thomas, G., and Brown, J.M. (2013). Mammalian alpha beta hydrolase domain (ABHD) proteins: Lipid metabolizing enzymes at the interface of cell signaling and energy metabolism. Biochim. Biophys. Acta *1831*, 792–802.
22. Xu, J., Gu, W., Ji, K., Xu, Z., Zhu, H., and Zheng, W. (2018). Sequence analysis and structure prediction of ABHD16A and the roles of the ABHD family members in human disease. Open Biol. *8*, 180017.

The American Journal of Human Genetics, Volume *108*

Supplemental information

ABHD16A deficiency causes a complicated form of hereditary spastic paraplegia associated with intellectual disability and cerebral anomalies

Gabrielle Lemire, Yoko A. Ito, Aren E. Marshall, Nicolas Chrestian, Valentina Stanley, Lauren Brady, Mark Tarnopolsky, Cynthia J. Curry, Taila Hartley, Wendy Mears, Alexa Derksen, Nadie Rioux, Nataly Laflamme, Harrol T. Hutchison, Lynn S. Pais, Maha S. Zaki, Tipu Sultan, Adrie D. Dane, Care4Rare Canada Consortium, Joseph G. Gleeson, Frédéric M. Vaz, Kristin D. Kernohan, Geneviève Bernard, and Kym M. Boycott

Figure S1: Lipidomics analysis of patient and control fibroblasts.

Lipidomics analysis of patient and control fibroblasts. The lipidome of four different patient fibroblasts (Individuals P3, P4, P7, P9) were compared with four independent control fibroblast lines. Boxplots of summed total levels of major lipid classes are shown for control (red) and patients (blue). Value on the y-axis are semi-quantitative lipid abundances (response of analyte divided by that of the internal standard multiplied by the concentration of the internal standard) PS and LPS are indicated in an orange box; PS is elevated in patients whereas LPS levels are not changed. In addition, changes in other lipid major classes were observed; PC, PE and different members of the ether lipid family (PC[O], PC[P], PE[O], PE[P]) are elevated in patients.

METHODS

Sequencing

The study was approved by the Children's Hospital of Eastern Ontario Research Ethics Board and institutional review boards of the University of California, San Diego. Informed consent was obtained from families. Exome sequencing of the six affected individuals from Family 1, 2 and 3 was performed in 2015 as part of the Care4Rare Canada research project (see Beaulieu *et al* [1] for technical details). Segregation of the *ABHD16A* variants in individuals from Family 1, 2 and 3 was performed by Sanger sequencing (primers available on request) at McGill University Health Center Research Institute (Montreal, QC, Canada). Trio exome sequencing of the proband and parents from Family 4 was performed by next-generation sequencing in a clinical laboratory. Family 4 was enrolled into the Care4Rare research program in 2019 after the clinical trio exome did not identify any variants to explain the proband's phenotype. The raw genomic data of these three family members were repatriated and processed through the Care4Rare Canada research bioinformatic pipeline. The four other affected individuals with homozygous variants in *ABHD16A* from Family 4 and 5 were identified via interrogation of the Geno2MP platform (Genotype to Mendelian Phenotype Browser, (URL:http://geno2mp.gs.washington.edu [(April, 2020) accessed])). Exome sequencing and data processing for these four individuals were performed by the Genomics Platform at the Broad Institute of MIT and Harvard (Cambridge, MA, USA) with an Illumina Nextera exome capture (~38 Mb target) and sequenced (150 bp paired reads) to cover >80% of targets at 20x and a mean target coverage of >100x. Exome sequencing data was processed through a pipeline based on Picard and mapping done using the BWA aligner to the human genome build 38. Variants were called using Genome Analysis Toolkit (GATK) HaplotypeCaller package version 3.5. Segregation of the *ABHD16A* variants in

individuals from Family 5 and 6 was performed by Sanger sequencing (primers available on request) at the Children's Hospital of Eastern Ontario (Ottawa, ON, Canada).

Patient fibroblast cell lines

Primary fibroblast cells from affected individuals P3 and P4 (Family 2) and P7 (Family 4) were derived and established from a skin biopsy by The Centre for Applied Genomics (Toronto, Canada). Primary fibroblast cells from affected individual P9 (Family 5) were derived and established from a skin biopsy at the University of California in San Diego (UCSD IRB protocol 171094, San Diego, USA) (see Chai *et al* [2] for further details).

RNA analysis

Total RNA was obtained from affected and control fibroblast cell lines with the RNeasy Mini Kit (QIAGEN) and reverse transcribed into complementary DNA (cDNA) with iScript kit (BioRad Laboratories) according to manufacturers' instructions. Control reactions without reverse transcriptase were prepared in parallel. cDNA was amplified with gene-specific primers and iQ SYBR Green Supermix (BioRad Laboratories) and read on a CFX96 Touch Real-time PCR Detection System (BioRad Laboratories). Gene expression was quantified using the standard Ct method with CFX software (BioRad Laboratories), and all data corrected against GAPDH as an internal control. The primer sequences used to amplify cDNA from exons 5-6 of NM_021160.2:

ABHD16A_ex4-5_F1 AAGTGGTGCCGTTTTCTCAC

ABHD16A_ex4-5_R1 ATGGTGATGAACTGCCGGTA

Fibroblast cell lines from five healthy, age and gender matched individuals were used as controls for the RT-PCR analysis (GM05381 (5-year-old male), GM07522 (19-year-old female),

GM07532 (16-year-old female), GM00038 (9-year-old female), GM00969 (2-year-old female) Coriell Institute, Hamden, USA).

Western blot analysis

Western blot analysis was conducted to assess protein levels in fibroblast cells derived from affected individuals and controls. Cells were lysed in radioimmunoprecipitation assay buffer containing 10 mg/mL each of aprotinin, phenylmethanesulfonyl fluoride, and leupeptin (all from Sigma) for 20 min at 4°C, followed by centrifugation at 13,000xg for 15 min and retrieval of supernatants. Total protein concentrations were determined by Bradford protein assay (BioRad Laboratories). Protein samples were resolved by SDS-PAGE, transferred onto nitrocellulose membrane and incubated in blocking solution (Tris-buffered saline (TBS), 5% non-fat milk, 0.1% Tween-20) for 1 h at room temperature followed by overnight incubation with primary antibody at 4°C (BAT5/ABHD16A, Abcam ab185549). Membranes were washed with TBS and 0.1% Tween-20 three times followed by incubation with secondary antibody (HRP conjugated anti-rabbit; BioRad Laboratories) for 1 h at room temperature. Blots were visualized by autoradiography using the Clarity Western ECL substrate (BioRad Laboratories). Fibroblast cell lines from five healthy, age and gender matched individuals were used as controls for the Western Blot analysis (GM01652 (11-year-old female), GM05381(5-year-old male), GM07522 (19-year-old female), GM07532 (16-year-old female), GM08399 (19-year-old female), Coriell Institute, Hamden, USA).

Proliferation assay

Fibroblast cells were plated in triplicate at a density of 3000 cells/well in 96 well dishes. 24 h later, wells were imaged for 72 h using the IncuCyte ZOOM and confluency was assessed using IncuCyte ZOOM confluence processing analysis tool.

Plasma sample collection

Whole blood drawn into EDTA containing tubes were collected from individuals P1 and P2, the unaffected sibling and both parents from Family 1. Whole blood samples were also collected from individuals P3 and P4 and both parents from Family 2. Medication and fasting details for each participant were collected at the time of blood draw. Blood tubes were kept on ice until centrifugation. They were centrifuged at 1500xg for 10 min at 4°C. The plasma was collected from the top layer, leaving behind the buffy coat and red blood cells. The samples were kept on ice during plasma collection. Four-hundred µL of plasma was then aliquoted into 2 pre-chilled vials and frozen immediately at -80°C.

Fibroblast cell culture for lipidomics assay

Cell lines for 4 patients (P3 and P4 (Family 2), P7 (Family 4), P9 (Family 5)) and five control cell lines (GM01652 (11-year-old female), GM05381(5-year-old male), GM07522 (19-year-old female), GM07532 (16-year-old female), GM08399 (19-year-old female), Coriell Institute, Hamden, USA) were grown in Ham's F10 Medium (Wisent Inc., St-Jean-Baptiste, Canada) supplemented with 10% fetal bovine serum (FBS; Sigma, St. Louis, USA), penicillin/streptomycin cocktail (Hyclone, Logan, USA) to a final concentration of 100 U/ml and L-glutamine (Hyclone, Logan, USA) to a final concentration of 2 mM. All cells were

treated in the same way to reduce variability including using the same lot number for media and its additives, the use of the same incubator, and same technician tending to the cells. When confluent, cells were maintained for another 8 days before collection. Stationary cells were harvested by trypsinization, washed twice with phosphate buffered saline and then washed with 0.9% saline before the cell pellet was frozen and stored at -80°C. An aliquot of each cell suspension was taken before the final pelleting and cell number obtained for normalization purposes. All cell pellets were collected on the same day.

Lipidomics assays

Frozen plasma and fibroblast cell pellets were shipped on dry ice to the Laboratory Genetic Metabolic Diseases, Amsterdam UMC, in Amsterdam for lipidomic analysis as previously described.[3]

REFERENCES

1. Beaulieu, C.L., Majewski, J., Schwartzentruber, J., Samuels, M.E., Fernandez, B.A., Bernier, F.P., Brudno, M., Knoppers, B., Marcadier, J., Dyment, D., et al. (2014). FORGE Canada Consortium: outcomes of a 2-year national rare-disease gene-discovery project. Am J Hum Genet. *94*, 809-817.
2. Chai, G., Webb, A., Li, C., Antaki, D., Lee, S., Breuss, M.W., Lang, N., Stanley, V., Anzenberg, P., Yang, X., et al. (2021). Mutations in Spliceosomal Genes PPIL1 and PRP17 Cause Neurodegenerative Pontocerebellar Hypoplasia with Microcephaly. Neuron. *109*, 241-256 e249.
3. Vaz, F.M., McDermott, J.H., Alders, M., Wortmann, S.B., Kolker, S., Pras-Raves, M.L., Vervaart, M.A.T., van Lenthe, H., Luyf, A.C.M., Elfrink, H.L., et al. (2019). Mutations in PCYT2 disrupt etherlipid biosynthesis and cause a complex hereditary spastic paraplegia. Brain. *142*, 3382-3397.